Acta Oncologica, 2014; 53: 580–589

informa
healthcare

REVIEW ARTICLE

Impacts of MR spectroscopic imaging on glioma patient management

IOANNA CHRONAIOU[1,2], ANNE LINE STENSJØEN[2], TORILL EIDHAMMER SJØBAKK[2], MORTEZA ESMAEILI[2] & TONE FROST BATHEN[2]

[1]*Radiography Department, Faculty of Technology (AFT), Sør-Trøndelag University College (HiST), Trondheim, Norway and* [2]*Department of Circulation and Medical Imaging, Norwegian University of Science and Technology (NTNU), Trondheim, Norway*

ABSTRACT

Magnetic resonance (MR) modalities are routine imaging tools in the diagnosis and management of gliomas. MR spectroscopic imaging (MRSI), which relies on the metabolic characteristics of tissues, has been developed to accelerate the understanding of gliomas and to aid in effective clinical decision making and development of targeted therapies. In this review, the potentials and practical challenges to frequently use this technique in clinical management of gliomas are discussed. The applications of new biomarkers detectable by MRSI in differential glioma diagnosis, pre- and post-treatment evaluations, and neurosurgery are also addressed.

Gliomas are classified into four grades (grade I–IV) according to the World Health Organization (WHO) criteria based on histology and biological behavior of the neoplasm [1]. Grade I gliomas are benign tumors, whereas grade II–IV are malignant tumors with increasing malignancy respectively. According to the WHO classification, grade I tumors have low mitotic activity. Grade II gliomas, low grade gliomas, are also characterized by low proliferative potential, but they are generally infiltrating into normal brain with a progression tendency towards more malignant features over time. Grade III gliomas have high mitotic activity and atypic cells and nucleuses. The most malignant gliomas are glioblastomas multiforme (GBM, WHO grade IV). GBMs are characterized by high proliferative activity, highly atypic cytoarchitecture and frequently necrotic areas, vascular thrombosis, and microvascular proliferation. Grades III and IV are considered as high-grade gliomas with a poor prognosis [2]. Current treatment for brain gliomas includes surgery followed by radiotherapy and/or chemotherapy depending on prognostic factors such as tumor location, glioma grade and histopathological features [3].

Conventional MR imaging (MRI) is a commonly used MR modality in tumor diagnostics and management. It provides anatomical information about a suspected lesion with relatively high spatial resolution and short scan time. Differences in the morphological structure of brain tumors are detected by MRI, and this is used for differential diagnosis and treatment assessment and follow-up. However, it is unreliable to determine tumor malignancy and evaluate therapy response solely based on morphology [4,5]. Diffuse tumors might not be visible in the anatomical MR images and response to therapy might be visible earlier as a molecular change than a morphological change. Thus, complementary information to the MRI may improve glioma patient management.

MR spectroscopy (MRS) can non-invasively map metabolic profiles and dynamics of the human brain [6,7]. A variety of metabolites can be detected (mM concentration range), and both steady state and kinetic analysis of cancer metabolism can be performed in vivo using ^{1}H (proton), ^{31}P (phosphorus) or ^{13}C (carbon) MRS [8,9]. Especially in the case of gliomas, the molecular information provided by

Correspondence: M. Esmaeili, Department of Circulation and Medical Imaging, Norwegian University of Science and Technology (NTNU), PO Box 8905, MTFS, 7491 Trondheim, Norway. Tel: + 47 45122970. E-mail: m.esmaeili@ntnu.no

(Received 15 November 2013; accepted 22 January 2014)

ISSN 0284-186X print/ISSN 1651-226X online © 2014 Informa Healthcare
DOI: 10.3109/0284186X.2014.891046

MRS combined with the anatomical information from MRI has been shown to improve initial diagnosis, tumor delineation for surgical or radiotherapy planning and post-therapy monitoring of tumor recurrence or progression to higher grade.

The purpose of this review is to highlight some of the expected impacts of MR spectroscopic imaging (MRSI) in clinical management of glioma patients. Furthermore, a short introduction to the MRSI technique and recent advances in this field are also included. Finally, the future direction, potentials and limitations of this technique will be discussed.

MRSI acquisition and processing techniques

In vivo MRS provides metabolic profiles of brain tumors non-invasively. MRS detects radiofrequency signals emitted from MR active nuclei, such as ^{1}H, ^{31}P, and ^{13}C, of different metabolites. The detected frequency of the metabolites is slightly different depending on their chemical microenvironment. This quality is described as 'chemical shift' and is expressed in a parts per million (ppm) scale with reference to a standard. For in vivo ^{1}H MRS, the water peak with a chemical shift value of 4.7 ppm is usually used as a standard reference signal. The intensity of the metabolite peak is proportional to the metabolite concentration level (Figure 1C). With localization determined from MR images, MR spectra are either detected from single volume elements (single voxel MRS) or from multiple volume elements (multivoxel) which is referred to as multivoxel MRSI or chemical shift imaging (CSI) (Figure 1A and B) [10]. The MRSI data can be visualized as color-coded metabolic or spectral maps (Figure 1D and E). The potential pitfall of conventional MRI in

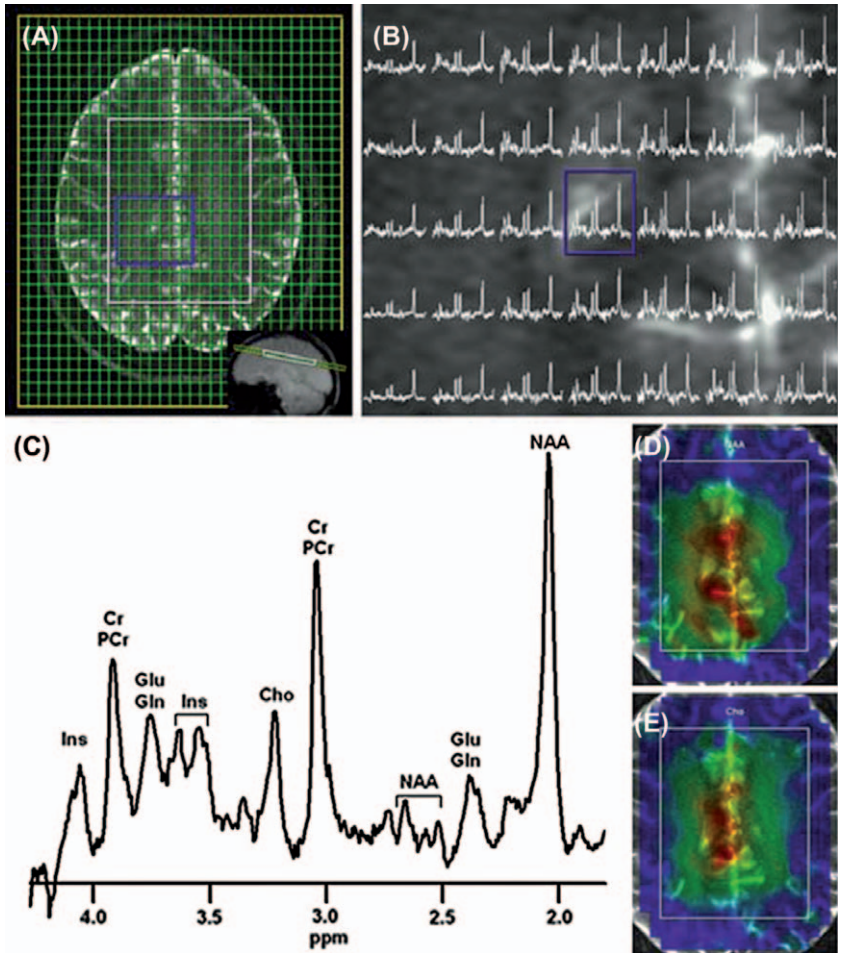

Figure 1. ^{1}H MRSI of the brain of a healthy volunteer at 7T. (A) The 2D MRSI matrix (green grid) is overlaid on a transverse T_2-weighted MR image and the MR spectra from the volume-of-interest (the white box in A) is shown on (B) with range 1.5–4.3 ppm. (C) The enlarged MR spectrum of the center voxel of the spectral map (blue voxel in B) shows the detectable metabolites in a healthy brain. The vertical axis represents signal intensities or concentrations of metabolites, while the horizontal axis represents chemical shifts (ppm). The assigned metabolites are; N-acetylaspartate (NAA), choline (Cho), glutamate (Glu), glutamine (Gln) creatine/phosphocreatine (Cr/PCr), and myo-inositol (Ins). (D, E) Color-coded metabolic maps calculated from the integration of Lorentzian fits to NAA and Cho. Adjusted with permission from [17].

discriminating between different tissue types might inherently lead to an inaccurate localization for single voxel MRS. The ability to acquire two dimensions (2D) or 3D metabolite distributions provides an assessment of heterogeneous tumor tissues [11].

MRSI pulse sequences use a combination of frequency and spatially selective pulses to suppress unwanted signals and localize the spatial extent and metabolic properties of specific regions of the anatomy. Acquisition parameters such as the used echo time (TE), the time between excitation and MR signal sampling, can greatly impact the metabolite signals. Commonly used TEs in the clinical setting are 30 ms (short TE), 144 ms (intermediate TE) or 270 ms (long TE). The use of short TE allows the detection of metabolites with both short and long T2 relaxation times (a time constant which reflects the MR signal decay), whereas use of long TE only allows detection of metabolites with long T2 relaxation times and therefore reduce the signal from lipids and other macromolecules. Intermediate TE results in an inverted lactate peak at 1.3 ppm, which is useful for lactate detection in some cases.

The commercially available and most commonly used MRSI sequence is point resolved spectroscopy (PRESS) [12] which provides reasonable scan times. PRESS is a localized double spin-echo pulse sequence. Recent advances in MRSI data acquisition have improved both the spatial and spectral resolution and the scanning time. Development of accelerated MRSI acquisitions is of particular interest in clinical applications. Echo planar spectroscopic imaging (EPSI) [13] and spiral-MRSI [14] are the most common fast MRSI techniques with comparable sensitivity per unit volume to that of PRESS. EPSI allows clinically feasible whole brain metabolite mapping at intermediate TEs [13], providing accelerated acquisition of spectral and spatial data simultaneously in shorter scan time. Another development in fast MRSI sequences has been the reduction in number of excitations by parallel imaging techniques such as sensitivity encoding (SENSE) [15] and generalized auto-calibrating partially parallel acquisitions (GRAPPA) [16].

Performing MRS at higher magnetic field strength (3T and beyond) improves the spectral resolution and sensitivity [17]. However, this is associated with technical challenges such as obtaining uniform excitation profiles and increased chemical shift displacement error (CSDE) [17]. To reduce the CSDE and establish uniform excitations, MRSI sequences with adiabatic pulses [18] such as localization by adiabatic selective refocusing (LASER) have been used [18]. LASER consists of a non-slice-selective adiabatic pulse to uniformly excite the volume of interest and three pairs of refocusing 180° adiabatic fully passage (AFP) pulses in three directions for localization. The first three pulses of the original fully adiabatic sequence in LASER were later replaced by a non-adiabatic optimized slice-selective excitation pulse in the semi-LASER sequence [19–21], which allows the use of shorter echo times than LASER (down to 30 ms at 3T). Edited MRSI sequences are able to detect specific metabolites that cannot be detected otherwise, such as recently shown for 2-hydroxyglutarate and lactate detection in glioma patients [22,23].

Quantitative analysis of the metabolites observed by MRSI is commonly performed using peak fitting or prior knowledge-based quantification. In the peak fitting method, peaks are initially selected and coarse estimations of the resonance frequency, line width, and peak intensity are made, either by the operator or by algorithms. Subsequently, a fit algorithm (such as the AMARES package in jMRUI [24]) is performed by using a least squares optimization algorithm, which iteratively fits all peaks to a line-shape model function. Prior knowledge about the metabolites detected in the spectra can also be incorporated in the fitting routine. The observed metabolites in the MR spectra are all characterized by signal parameters such as relative amplitude, frequency, phase, and resonance chemical shift. These spectral parameters are known from previous ^{1}H MRS brain studies, and can be used as prior knowledge to simulate the metabolite resonances considering the acquisition parameters such as magnetic field strength, pulse sequence, echo and repetition times, and pH. The simulated resonances from metabolites of interest can also be combined to generate a basis set for spectral fitting. LCModel [25] analyzes the MRS data automatically by iteratively fitting the experimentally obtained MR spectra with the determined basis set using least squares optimization, whereas jMRUI [26] provides both a semi-automatic peak fitting technique (AMARES) and a fully automatic fitting routine (QUEST) using metabolite basis sets [27].

MRSI of brain tumors

In the last two decades a lot of effort has been made to understand the biological mechanisms underlying brain gliomas. Metabolites are the downstream products from preceding gene and protein activity, and thereby close measures of the phenotype under investigation. Changes in metabolite levels will indicate which biological pathways are affected under certain conditions. Metabolites that serve as objective indicators of normal biological and pathogenic processes or pharmacological responses to a therapeutic intervention can be established as biomarkers. None of the metabolites mentioned in the next paragraph are tumor specific, in the sense that they

can be observed both in normal brain as well as tumor tissue. However, changes in the metabolite concentrations or metabolite ratios between normal and tumor tissue can prove malignancy. Metabolites frequently observed in gliomas are given in Table I.

Cancer cells have a higher rate of glycolysis (energy production process) than normal cells (known as The Warburg effect) [28]. Metabolites associated with the glycolytic pathway (lactate, alanine, lipids, and pyruvate) are suggested as biomarkers of abnormal energy metabolism [29]. Lactate is related to hypoxia and necrosis, and can be observed in higher grade tumors [28]. Lipids are observed in necrosis and are also related to hypoxia and apoptosis [28,30]. Phospholipid metabolism is commonly altered in cancer cells [31], and is associated with cellular proliferation, apoptosis, tumor progression, angiogenesis, oncogenic signaling pathways, and cell survival [32]. Choline containing compounds are the downstream products of phospholipid metabolism. Total choline (tCho) is a composite signal, and includes the choline containing compounds [choline (Cho), phosphocholine (PCho), and glycerophosphocholine (GPC)] that can be detected individually with high resolution in vitro and ex vivo MRS [33]. The tCho level has been found to be abnormally high in a variety of tumors [7,32] and tCho has been suggested as a biomarker of cell density and rapid cell membrane turnover [34,35]. The tCho level in tumor tissue might also reflect the amount of fiber destruction of gliomas [36].

N-acetyl aspartate (NAA) is another important metabolite in ^{1}H MR spectra of the brain and is known as a marker of neuronal activity [37]. A decrease in NAA has been repeatedly observed in different brain tumors [7]. Total creatine (tCr), myo-Inositol (mI) and glycine (Gly) are also detected in ^{1}H MR spectra of brain tumors. tCr includes creatine and phosphocreatine and indicates the intracellular energy states [38]. The relatively increased myo-Inositol and glutamine in the contralateral normal appearing white matter of GBM patients have been suggested as markers of early neoplastic infiltrations [39]. Gly has been reported as a marker of tumor malignancy [40]. In general, gliomas show elevated tCho and reduced NAA and tCr compared to normal brain tissue and possibly elevated lactate and lipids in the necrotic areas [41]. Figure 2 shows the difference in metabolite concentrations between a glioma spectrum and a normal brain spectrum.

A new and promising biomarker, the oncometabolite 2-hydroxyglutarate (2-HG) has been discovered in a subtype of gliomas by ^{1}H MRS using clinical scanners (3 T) [22,42,43]. 2-HG has been detected in glioma patients harboring *IDH*-mutations. *IDH1*/*IDH2* mutations are present in about 80% of WHO grade II and III gliomas and in certain GBM subtypes [43], but only in less than 10% of primary

Table I. Biochemical features of brain gliomas detectable by ^{1}H-MRSI.

Metabolite	Spectrum peak	Characteristics
N-acetyl aspartate (NAA)	Singlet at 2.01 ppm	– marker of neuronal activity [37] – absent in metastatic and non-neuronal brain tumors [7] – reduced in infiltrative tumors (such as gliomas) compared to normal tissue [7]
Total choline (tCho)	Singlet at 3.22 ppm	– marker of phospholipid turnover in membrane [32] – reflects cellular proliferation [34,48] – indicator of progression in gliomas [35]
Phosphocreatine and creatine (tCr)	Singlets at 3.03 ppm and 3.9 ppm	– related to cellular energy metabolism [38] – prognostic factor in low-grade gliomas [38]
Myo-inositol (mI)	Multiplets as a single peak at 3.56 ppm [40]	– marker of early neoplastic infiltrations in GBMs [39]
Glycine (Gly)	Singlet at 3.56 ppm [40]	– increased in malignant gliomas [40]
Glutamate, glutamine (Glx)	Broad multiplet signals between 2 and 2.4 ppm and ≈3.8 ppm	– present predominantly in astrocytes [39] – marker of early neoplastic infiltrations in GBMs, when found in increased concentrations in normal-appearing white matter (NAWM) [39]
Lactate	Doublet at 1.33 ppm	– related with necrosis [30] and hypoxia [28] – more often observed at higher grade tumors [28] – regulator of energy flux within the cancerous cells [28]
Lipids	0.9 and 1.3 ppm	– related with necrosis [30] – more often observed at higher grade tumors [28] – regulator of energy flux within the cancerous cells [28]
Alanine (Ala)	Doublet at 1.47 ppm	– increased concentration in hypoxic tissue [28] – regulator of energy flux within the cancerous cells [28]
2-hydroxyglutarate (2-HG)	Multiplets at 1.85 ppm, 2.01 ppm, 2.28 ppm, and 4.05 ppm	– oncometabolite that can be found in gliomas with an *IDH*-mutation [22,42,43]

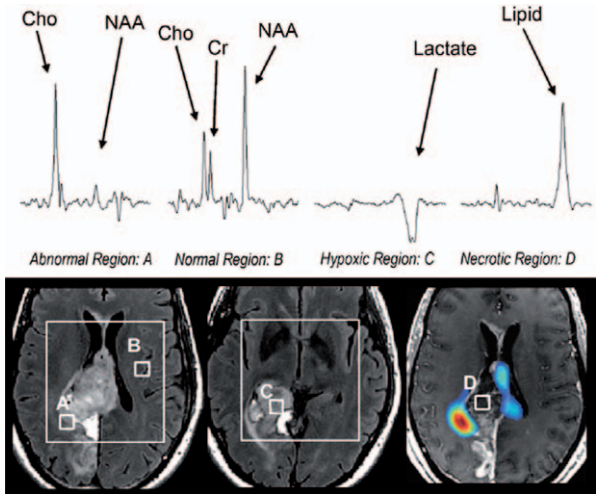

Figure 2. ^{1}H MRSI spectra from a GBM patient overlayed on anatomical MR images, from left to right; T2-FLAIR images with the PRESS-selected volume superimposed on two different axial slices and T1-weighted post-gadolinium image with a superimposed color-coded Cho/NAA overlay map, shows extreme heterogeneity of the tumor. Localized metabolic information from different regions of the brain indicated an abnormal region (A) with high level of Cho/NAA ratio and lack of Cr signal compared to the normal region (B). The hypoxic (C) and necrotic (D) regions show elevated lactate and lipid respectively compared to the normal region. These regions are not distinguishable from anatomical MR images alone. Illustrated with permission from [41].

GBMs [44]. There are growing evidence that these mutations may play an important role in the development of gliomas [45]. The *IDH*-mutation status is an important prognostic marker, as patients with *IDH*-mutated gliomas have significantly better overall survival than patients without this mutation [46]. *IDH* mutations lead to increased levels of 2-HG, and detection of 2-HG by MRS can become a non-invasive method of evaluating *IDH* mutation status [22].

The detection of some metabolites mentioned above is not feasible with commercially available sequences and might need appropriate post-processing routines. This limitation is due to the overlapping signals in proton spectra such as the mI and Gly or choline containing signals. Other MRS techniques such as ^{31}P- and ^{13}C-MRS provide wider chemical shift dispersion, thereby, better spectral resolution than ^{1}H MRS. ^{31}P-containing metabolites such as PCho, GPC, phosphoethanolamine (PEtn), and glycerophosphoethanolamine (GPE) can be directly detected by ^{31}P MRSI [47]. PEtn and GPE are involved in phospholipid metabolism, along with the choline containing metabolites [48]. In vivo ^{13}C MRS detects concentrations above 0.1 mM of metabolites such as glutamine, glutamate, and NAA. However, most commercial MR scanners are generally only capable of proton spectroscopy and, therefore, ^{31}P/^{13}C MRSI of gliomas are less studied.

Value of MRSI in glioma clinical practice

Gliomas are infiltrative and heterogeneous tumors. ^{1}H MRSI is an especially useful technique to study metabolism in normal and heterogeneous tumor tissues in brain gliomas, with ability to detect chemical differences between the two. Many studies have shown that MRSI can aid the accurate diagnosis, treatment planning, and therapy response evaluation of gliomas. Relatively lower sensitivity of MRSI, compared to the conventional MRI, is the main challenge for including this technique to clinical routines. The lower sensitivity hamper the spatial resolution of MRSI (nominal voxel size ~10 mm^3) compared to what can be achieved with other MR techniques, such as conventional MRI (nominal voxel size ~1 mm^3), diffusion-weighted and perfusion imaging (nominal voxel size ~2 mm^3). Advances in MR technology, however, may allow a more frequent use of MRSI in the clinical management of brain gliomas as an additional tool to conventional MRI. Access to higher magnetic field strengths can greatly improve the sensitivity, and therefore the spatial resolution, of MRSI. Diagnostic accuracy in glioma grading was improved using MRSI alone or by combination with other MR modalities [5,49,50]. Therefore, this technique has been suggested as a useful tool in glioma management. In clinical practice, it is important that relevant MRSI results become available rapidly and reliably, and there are still limitations which may discourage the widespread acceptance of MRSI in clinical routine such as: 1) a lack of standardization in analyzing MRSI data, which may rely heavily on modeling and on a priori information; 2) application challenges; Radiologist are less familiar with the technical issues of MRSI or interpretation of MRS data, which require special training and developments in MRS data visualization; 3) the wide range of MRSI techniques that are used for clinical applications, which makes comparisons between studies challenging.

Differential diagnosis: Non-invasive grading of gliomas

According to the European guidelines form 2010, surgery is recommended as a primary treatment for low grade gliomas, together with radiotherapy in patients with negative prognostic factors [51]. Grade III gliomas are all treated with initial surgery when possible, which is generally followed by radiotherapy, and in some cases by chemotherapy [52,53]. Aggressive extent of resection of tumor tissues is highly advised for GBM patients, as it is associated with a better survival [54]. Since high grade gliomas receive different treatment and have different prognosis than low grade gliomas, accurate grading of gliomas has high impact on clinical management of gliomas.

Based on the different metabolic profiles of high and low grade gliomas, it is possible to discriminate high from low grade gliomas non-invasively using multivoxel MRSI. Many metabolites and metabolite ratios have been reported to have the ability (high sensitivity and specificity) to differentiate between high and low grade gliomas, such as the maximum or mean value over the tumor of tCho [55], tCho/NAA [56,57], tCho/tCr, [56,57], or the minimum value of NAA/tCr [57]. Although MRSI cannot replace histopathologic analysis in the clinical practice, it can assist in glioma grading in cases where conventional MR cannot yield diagnosis [58], either on its own or combined with perfusion and diffusion imaging as part of multi-parametric MR assessment of gliomas [57,59]. Combination of MRS and perfusion imaging can improve the discrimination accuracy between high and low grade gliomas up to 100% [60,61].

Treatment planning, radiotherapy, stereotactic biopsy, and image-guided surgery

Gliomas display highly heterogeneous features with regions of tumor, edema, and where tumor and edema co-exist. They can also include regions displaying several tumor grades. Histopathological grading of gliomas depends strongly on the biopsy site. ^{1}H MRSI can suggest the most malignant part of the tumor for biopsy targeting, increasing the possibility for accurate tumor grading. Additionally, a pre-operative mapping of the most malignant part of the gliomas can greatly aid a precise lesion resection and improve the post-therapy decision making. High spatial resolution ^{1}H-MRSI, that can be achieved in a 3T scanner, can provide differential metabolic mapping of the brain and improve the delineation of brain tumors [50,62].

Radiotherapy planning, stereotactic biopsy planning and image-guided surgery require accurate knowledge of the true margins of the tumor. In conventional MR images, contrast enhancement can depict active tumor, necrosis, or radiation-induced changes, however, the infiltrative region may remain concealed [50,63,64]. Therefore, conventional MRI may lead to inaccurate estimation of the tumor spatial extent. Integration of MRI parameters such as conventional T2-weighted imaging to MRSI was examined in pre-operation planning of glioma patients [65–67] (Figure 3). MRSI can classify pre-enhancing regions into infiltrative tissue, vasogenic edema and edematous infiltrative tissues, when

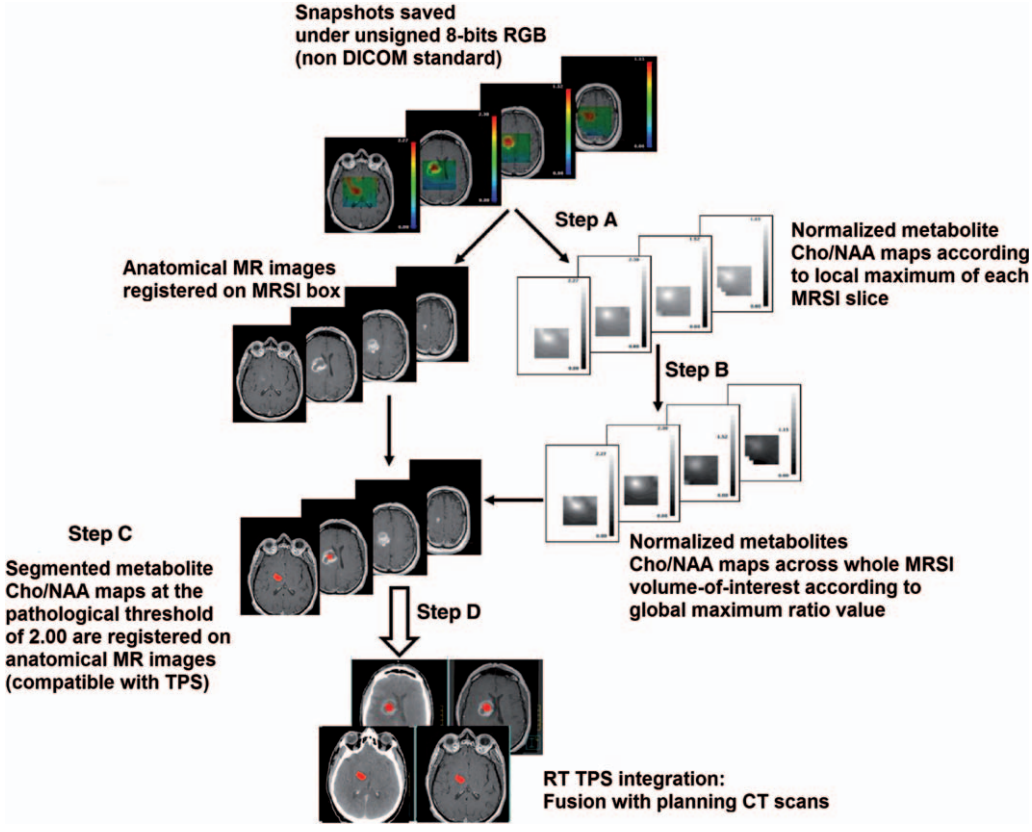

Figure 3. The flowchart demonstrates a proposed post-processing method which integrates MRSI-defined regions with abnormal Cho/NAA ratios into a radiotherapy treatment planning system. Adapted with permission from [67].

combined with perfusion and diffusion imaging [60]. Specifically, tumor, edema, and the combination of them have different characteristics that can be detected by tCho/NAA ratio, apparent diffusion coefficient, and relative cerebral blood volume [60]. On its own, MRSI can improve accurate tumor delineation [65] and segmentation [68] compared to conventional MRI, based on the tCho/NAA levels.

The combination of MRSI data with anatomical MRI can help in tumor segmentation and consequently in targeting the most malignant part of the tumor during stereotactic biopsy targeting [62]. Automatic tumor segmentation have been achieved based on the assumption that the tCho/NAA ratio follows a Gaussian distribution in the normal brain [66]. The image of the segmented tumor was then combined with anatomical MR data and the resulting image was used for intraoperative ^{1}H-MR spectroscopic navigation. With regards to radiotherapy planning, the tCho/NAA ratio map can be integrated reliably to the treatment planning system to aid radiotherapy planning [67]. It has also been suggested that MRSI can predict the location of a post-radiotherapy relapse [69].

Response to therapy

The treatment of gliomas includes surgical removal, radiotherapy, chemotherapy and administration of novel biological drugs. Response to treatment is currently evaluated by assessing the diameter or the volume of the contrast-enhanced lesion in the anatomical MR images [70]. The inability of conventional MRI to accurately estimate the tumor extent, may hamper the response evaluations. For example, in case of radiotherapy, response evaluations are often associated to discrimination between post-treatment radiation effects and recurrent tumor [71]. Both post-treatment radiation effects and tumor recurrence might be misinterpreted by conventional MRI because of their resembling pathological symptoms [4,72,73]. Metabolic biomarkers are thought to be more specific and sensitive in monitoring tumor evolutions and/or treatment response [74]. ^{1}H MRSI has potential in differentiating recurring tumor from post-treatment radiation effects [72]. Specifically, the tCho/NAA, tCho/tCr, and NAA/tCr metabolite ratios from voxels within the suspected lesion (contrast enhanced area) could differentiate tumor from radiation injury [11,73,75]. Higher tCho/NAA and tCho/tCr ratios were found in recurrent tumor than in radiation necrosis and a significant decrease in NAA/tCr was found in tumor as compared with radiation injury [11,73,75]. The differences in these metabolite ratios between recurrent tumor and radiation injury has been noted in many studies, however, there is a limited knowledge of the underlying biological mechanisms [76].

Biological drugs have been used in treatment trials for brain gliomas and include chemotherapy and anti-angiogenic drugs. Anti-angiogenic drugs target several pathways [77]. When measured by contrast-enhanced anatomical MRI, changes to tumor size reflect 'pseudo-response' and not normalization of tumor vasculature. ^{1}H and ^{31}P MRSI can be used in monitoring early response to anti-angiogenic therapy in order to determine how successful the therapy is and decide on additional treatment [78,79]. tCho/tCr, NAA/tCr and NAA/tCho metabolite ratios that were acquired with ^{1}H MRSI were able to discriminate between different prognostic groups and metabolites NAA and tCho were noted as useful biomarkers in the evaluation of treatment with anti-angiogenic drugs [79]. Apart from ^{1}H MRSI, ^{31}P MRSI was used to test the efficacy of anti-angiogenic treatment in glioma patients by detecting changes in the phospholipid metabolism of gliomas before and under anti-angiogenic treatment [74]. Hyperpolarized ^{13}C MRS has promising results in studying tumor metabolism and evaluating response to chemotherapy and anti-angiogenic drugs in xenograft models [80,81].

Conclusions and future directions

MRSI is a promising MR modality in pre- and post-surgical management of brain tumors. Developments in MR technology render MRS-based methods in pre- and post-surgical scanning routine of glioma patients feasible. ^{1}H MRSI can be used for differential diagnosis of the glioma, identification of the true tumor margins and the most malignant part of the tumor and post-therapy evaluation. Research focus on reliable automation procedures for post-processing of the MRSI raw data to enable rapid and robust visualization for the radiologist will be important to enhance the use of MRSI in clinical routine. Other translational challenges of the MRSI technique, such as the relatively lower spatial resolution and sensitivity than anatomical MRI techniques, are logical targets for optimization and subjects of high field MR research.

Declaration of interest: The authors report no conflicts of interest. The authors alone are responsible for the content and writing of the paper.

References

[1] Louis DN. WHO classification of tumours of the central nervous system. Geneva, Switzerland: World Health Organization; 2007.

[2] Taylor LP. Diagnosis, treatment, and prognosis of glioma: Five new things. Neurology 2010;75(18 Suppl 1):S28–32.
[3] Buckner JC. Factors influencing survival in high-grade gliomas. Semin Oncol 2003;30:10–4.
[4] Shah R, Vattoth S, Jacob R, Manzil FFP, O'Malley JP, Borghei P, et al. Radiation necrosis in the brain: Imaging features and differentiation from tumor recurrence. Radiographics 2012;32:1343–59.
[5] Law M, Yang S, Wang H, Babb JS, Johnson G, Cha S, et al. Glioma grading: Sensitivity, specificity, and predictive values of perfusion MR imaging and proton MR spectroscopic imaging compared with conventional MR imaging. Am J Neuroradiol 2003;24:1989–98.
[6] Nelson SJ. Multivoxel magnetic resonance spectroscopy of brain tumors. Mol Cancer Ther 2003;2:497–507.
[7] Howe FA, Opstad KS. 1H MR spectroscopy of brain tumours and masses. NMR Biomed 2003;16:123–31.
[8] Kurhanewicz J, Vigneron DB, Brindle K, Chekmenev EY, Comment A, Cunningham CH, et al. Analysis of cancer metabolism by imaging hyperpolarized nuclei: Prospects for translation to clinical research. Neoplasia 2011;13:81–97.
[9] Pinker K, Stadlbauer A, Bogner W, Gruber S, Helbich TH. Molecular imaging of cancer: MR spectroscopy and beyond. Eur J Radiol 2012;81:566–77.
[10] De Graaf RA. In vivo NMR spectroscopy – principles and techniques, 2nd ed. Chichester, UK: John Wiley & Sons, Ltd; 2007.
[11] Zeng QS, Li CF, Zhang K, Liu H, Kang XS, Zhen JH. Multivoxel 3D proton MR spectroscopy in the distinction of recurrent glioma from radiation injury. J Neurooncol 2007;84:63–9.
[12] Bottomley PA. Spatial localization in NMR spectroscopy in vivo. Ann N Y Acad Sci 1987;508:333–48.
[13] Posse S, DeCarli C, Le Bihan D. Three-dimensional echo-planar MR spectroscopic imaging at short echo times in the human brain. Radiology 1994;192:733–8.
[14] Adalsteinsson E, Irarrazabal P, Topp S, Meyer C, Macovski A, Spielman DM. Volumetric spectroscopic imaging with spiral-based k-space trajectories. Magn Reson Med 1998; 39:889–98.
[15] Lin FH, Tsai SY, Otazo R, Caprihan A, Wald LL, Belliveau JW, et al. Sensitivity-encoded (SENSE) proton echo-planar spectroscopic imaging (PEPSI) in the human brain. Magn Reson Med 2007;57:249–57.
[16] Zhu X, Ebel A, Ji JX, Schuff N. Spectral phase-corrected GRAPPA reconstruction of three-dimensional echo-planar spectroscopic imaging (3D-EPSI). Magn Reson Med 2007;57:815–20.
[17] Scheenen TW, Heerschap A, Klomp DW. Towards 1H-MRSI of the human brain at 7T with slice-selective adiabatic refocusing pulses. Magma 2008;21:95–101.
[18] Garwood M, DelaBarre L. The return of the frequency sweep: Designing adiabatic pulses for contemporary NMR. J Magn Reson 2001;153:155–77.
[19] Scheenen TW, Klomp DW, Wijnen JP, Heerschap A. Short echo time 1H-MRSI of the human brain at 3T with minimal chemical shift displacement errors using adiabatic refocusing pulses. Magn Reson Med 2008;59:1–6.
[20] Kobus T, Wright AJ, Van Asten JJ, Heerschap A, Scheenen TW. In vivo (1) H MR spectroscopic imaging of aggressive prostate cancer: Can we detect lactate? Magn Reson Med 2014;71:26–34.
[21] Wijnen JP, Idema AJ, Stawicki M, Lagemaat MW, Wesseling P, Wright AJ, et al. Quantitative short echo time 1H MRSI of the peripheral edematous region of human brain tumors in the differentiation between glioblastoma, metastasis, and meningioma. J Magn Reson Imaging 2012;36:1072–82.
[22] Choi C, Ganji SK, DeBerardinis RJ, Hatanpaa KJ, Rakheja D, Kovacs Z, et al. 2-hydroxyglutarate detection by magnetic resonance spectroscopy in IDH-mutated patients with gliomas. Nat Med 2012;18:624–9.
[23] Park I, Chen AP, Zierhut ML, Ozturk-Isik E, Vigneron DB, Nelson SJ. Implementation of 3 T lactate-edited 3D 1H MR spectroscopic imaging with flyback echo-planar readout for gliomas patients. Ann Biomed Eng 2011;39:193–204.
[24] Vanhamme L, van den Boogaart A, Van Huffel S. Improved method for accurate and efficient quantification of MRS data with use of prior knowledge. J Magn Reson 1997;129: 35–43.
[25] Provencher SW. Estimation of metabolite concentrations from localized in vivo proton NMR spectra. Magn Reson Med 1993;30:672–9.
[26] Naressi A, Couturier C, Devos JM, Janssen M, Mangeat C, de Beer R, et al. Java-based graphical user interface for the MRUI quantitation package. Magma 2001;12:141–52.
[27] Ratiney H, Coenradie Y, Cavassila S, van Ormondt D, Graveron-Demilly D. Time-domain quantitation of 1H short echo-time signals: Background accommodation. Magma 2004;16:284–96.
[28] Kounelakis MG, Zervakis ME, Postma GJ, Buydens LMC, Heerschap A, Kotsiakis X. Validation of MRS metabolic markers in the classification of brain gliomas and their correlation to energy metabolism. IFMBE Proc 2010;29:33–6.
[29] Kounelakis M, Zervakis M, Giakos G, Postma G, Buydens L, Kotsiakis X. On the relevance of glycolysis process on brain gliomas. IEEE Trans Inf Technol Biomed 2013; 17:128–35.
[30] Yaman E, Buyukberber S, Benekli M, Oner Y, Coskun U, Akmansu M, et al. Radiation induced early necrosis in patients with malignant gliomas receiving temozolomide. Clin Neurol Neurosurg 2010;112:662–7.
[31] Ackerstaff E, Glunde K, Bhujwalla ZM. Choline phospholipid metabolism: A target in cancer cells? J Cell Biochem 2003;90:525–33.
[32] Glunde K, Bhujwalla ZM, Ronen SM. Choline metabolism in malignant transformation. Nat Rev Cancer 2011;11: 835–48.
[33] Vettukattil R, Gulati M, SjøbakkTE, Jakola AS, Kvernmo NA, Torp SH, et al. Differentiating diffuse World Health Organization grade II and IV astrocytomas with ex vivo magnetic resonance spectroscopy. Neurosurgery 2013;72:186–95; discussion 95.
[34] Tamiya T, Kinoshita K, Ono Y, Matsumoto K, Furuta T, Ohmoto T. Proton magnetic resonance spectroscopy reflects cellular proliferative activity in astrocytomas. Neuroradiology 2000;42:333–8.
[35] Tedeschi G, Lundbom N, Raman R, Bonavita S, Duyn JH, Alger JR, et al. Increased choline signal coinciding with malignant degeneration of cerebral gliomas: A serial proton magnetic resonance spectroscopy imaging study. J Neurosurgery 1997;87:516–24.
[36] Stadlbauer A, Hammen T, Buchfelder M, Bachmair J, Dorfler A, Nimsky C, et al. Differences in metabolism of fiber tract alterations in gliomas: A combined fiber density mapping and magnetic resonance spectroscopic imaging study. Neurosurgery 2012;71:454–63.
[37] Ebisu T, Rooney WD, Graham SH, Weiner MW, Maudsley AA. N-acetylaspartate as an in vivo marker of neuronal viability in kainate-induced status epilepticus: 1H magnetic resonance spectroscopic imaging. J Cereb Blood Flow Metab 1994; 14:373–82.
[38] Hattingen E, Raab P, Franz K, Lanfermann H, Setzer M, Gerlach R, et al. Prognostic value of choline and creatine in WHO grade II gliomas. Neuroradiology 2008;50:759–67.

[39] Kallenberg K, Bock HC, Helms G, Jung K, Wrede A, Buhk JH, et al. Untreated glioblastoma multiforme: Increased myo-inositol and glutamine levels in the contralateral cerebral hemisphere at proton MR spectroscopy. Radiology 2009;253:805–12.

[40] Hattingen E, Lanfermann H, Quick J, Franz K, Zanella FE, Pilatus U. 1H MR spectroscopic imaging with short and long echo time to discriminate glycine in glial tumours. Magma 2009;22:33–41.

[41] Osorio JA, Ozturk-Isik E, Xu D, Cha S, Chang S, Berger MS, et al. 3D 1H MRSI of brain tumors at 3.0 Tesla using an eight-channel phased-array head coil. J Magn Reson Imaging 2007;26:23–30.

[42] Andronesi OC, Kim GS, Gerstner E, Batchelor T, Tzika AA, Fantin VR, et al. Detection of 2-hydroxyglutarate in IDH-mutated glioma patients by in vivo spectral-editing and 2D correlation magnetic resonance spectroscopy. Sci Transl Med. 2012;4:116ra4.

[43] Pope WB, Prins RM, Albert Thomas M, Nagarajan R, Yen KE, Bittinger MA, et al. Non-invasive detection of 2-hydroxyglutarate and other metabolites in IDH1 mutant glioma patients using magnetic resonance spectroscopy. J Neurooncol 2012;107:197–205.

[44] Esmaeili M, Vettukattil R, Bathen TF. 2-hydroxyglutarate as a magnetic resonance biomarker for glioma subtyping. Transl Oncol 2013;6:92–8.

[45] Cohen AL, Holmen SL, Colman H. IDH1 and IDH2 mutations in gliomas. Curr Neurol Neurosci Rep 2013;13:345.

[46] Christensen BC, Smith AA, Zheng S, Koestler DC, Houseman EA, Marsit CJ, et al. DNA methylation, isocitrate dehydrogenase mutation, and survival in glioma. J Natl Cancer Inst 2011;103:143–53.

[47] Klomp DW, Wijnen JP, Scheenen TW, Heerschap A. Efficient 1H to 31P polarization transfer on a clinical 3T MR system. Magn Reson Med 2008;60:1298–305.

[48] Podo F. Tumour phospholipid metabolism. NMR Biomed 1999;12:413–39.

[49] Server A, Kulle B, Gadmar OB, Josefsen R, Kumar T, Nakstad PH. Measurements of diagnostic examination performance using quantitative apparent diffusion coefficient and proton MR spectroscopic imaging in the preoperative evaluation of tumor grade in cerebral gliomas. Eur J Radiol 2011;80:462–70.

[50] Li Y, Lupo JM, Parvataneni R, Lamborn KR, Cha S, Chang SM, et al. Survival analysis in patients with newly diagnosed glioblastoma using pre- and postradiotherapy MR spectroscopic imaging. Neuro Oncol 2013;15:607–17.

[51] Soffietti R, Baumert BG, Bello L, von Deimling A, Duffau H, Frenay M, et al. Guidelines on management of low-grade gliomas: Report of an EFNS-EANO Task Force. Eur J Neurol 2010;17:1124–33.

[52] Stupp R, Tonn J-C, Brada M, Pentheroudakis G on behalf of the ESMO Guidelines Working Group. High-grade malignant glioma: ESMO clinical practice guidelines for diagnosis, treatment and follow-up. Ann Oncol 2010;21(Suppl 5): v190–3.

[53] Brem SS, Bierman PJ, Brem H, Butowski N, Chamberlain MC, Chiocca EA, et al. Central nervous system cancers. J Natl Compr Canc Netw 2011;9:352–400.

[54] Sanai N, Polley MY, McDermott MW, Parsa AT, Berger MS. An extent of resection threshold for newly diagnosed glioblastomas. J Neurosurg 2011;115:3–8.

[55] Senft C, Hattingen E, Pilatus U, Franz K, Schanzer A, Lanfermann H, et al. Diagnostic value of proton magnetic resonance spectroscopy in the noninvasive grading of solid gliomas: Comparison of maximum and mean choline values. Neurosurgery 2009;65:908–13; discussion 13.

[56] Zeng Q, Liu H, Zhang K, Li C, Zhou G. Noninvasive evaluation of cerebral glioma grade by using multivoxel 3D proton MR spectroscopy. Magn Reson Imaging 2011;29: 25–31.

[57] Yang D, Korogi Y, Sugahara T, Kitajima M, Shigematsu Y, Liang L, et al. Cerebral gliomas: Prospective comparison of multivoxel 2D chemical-shift imaging proton MR spectroscopy, echoplanar perfusion and diffusion-weighted MRI. Neuroradiology 2002;44:656–66.

[58] Setzer M, Herminghaus S, Marquardt G, Tews DS, Pilatus U, Seifert V, et al. Diagnostic impact of proton MR-spectroscopy versus image-guided stereotactic biopsy. Acta Neurochir (Wien) 2007;149:379–86.

[59] Catalaa I, Henry R, Dillon WP, Graves EE, McKnight TR, Lu Y, et al. Perfusion, diffusion and spectroscopy values in newly diagnosed cerebral gliomas. NMR Biomed 2006; 19:463–75.

[60] Di Costanzo A, Scarabino T, Trojsi F, Giannatempo GM, Popolizio T, Catapano D, et al. Multiparametric 3T MR approach to the assessment of cerebral gliomas: Tumor extent and malignancy. Neuroradiology 2006;48:622–31.

[61] Zonari P, Baraldi P, Crisi G. Multimodal MRI in the characterization of glial neoplasms: The combined role of single-voxel MR spectroscopy, diffusion imaging and echo-planar perfusion imaging. Neuroradiology 2007; 49:795–803.

[62] Stadlbauer A, Moser E, Gruber S, Buslei R, Nimsky C, Fahlbusch R, et al. Improved delineation of brain tumors: an automated method for segmentation based on pathologic changes of 1H-MRSI metabolites in gliomas. Neuroimage 2004;23:454–61.

[63] Chan AA, Lau A, Pirzkall A, Chang SM, Verhey LJ, Larson D, et al. Proton magnetic resonance spectroscopy imaging in the evaluation of patients undergoing gamma knife surgery for Grade IV glioma. J Neurosurg 2004;101:467–75.

[64] Hamans B, Navis AC, Wright A, Wesseling P, Heerschap A, Leenders W. Multivoxel (1)H MR spectroscopy is superior to contrast-enhanced MRI for response assessment after anti-angiogenic treatment of orthotopic human glioma xenografts and provides handles for metabolic targeting. Neuro Oncol 2013;15:1615–24.

[65] Ganslandt O, Stadlbauer A, Fahlbusch R, Kamada K, Buslei R, Blumcke I, et al. Proton magnetic resonance spectroscopic imaging integrated into image-guided surgery: Correlation to standard magnetic resonance imaging and tumor cell density. Neurosurgery 2005;56(2 Suppl):291–8; discussion 298.

[66] Stadlbauer A, Moser E, Gruber S, Nimsky C, Fahlbusch R, Ganslandt O. Integration of biochemical images of a tumor into frameless stereotaxy achieved using a magnetic resonance imaging/magnetic resonance spectroscopy hybrid data set. J Neurosurg 2004;101:287–94.

[67] Ken S, Vieillevigne L, Franceries X, Simon L, Supper C, Lotterie JA, et al. Integration method of 3D MR spectroscopy into treatment planning system for glioblastoma IMRT dose painting with integrated simultaneous boost. Radiat Oncol 2013;8:1.

[68] Ganslandt O, Stadlbauer A. Infiltration zone in glioma: Proton magnetic resonance spectroscopic imaging. In: Hayat MA, editor. Tumors of the central nervous system, volume 1. Netherlands: Springer; 2011. p. 81–8.

[69] Laprie A, Catalaa I, Cassol E, McKnight TR, Berchery D, Marre D, et al. Proton magnetic resonance spectroscopic imaging in newly diagnosed glioblastoma: Predictive value for the site of postradiotherapy relapse in a prospective longitudinal study. Int J Radiat Oncol Biol Phys 2008;70: 773–81.

[70] Wen PY, Macdonald DR, Reardon DA, Cloughesy TF, Sorensen AG, Galanis E, et al. Updated response assessment criteria for high-grade gliomas: Response assessment in neuro-oncology working group. J Clin Oncol 2010;28: 1963–72.

[71] Fink JR, Carr RB, Matsusue E, Iyer RS, Rockhill JK, Haynor DR, et al. Comparison of 3 Tesla proton MR spectroscopy, MR perfusion and MR diffusion for distinguishing glioma recurrence from posttreatment effects. J Magn Reson Imaging 2012;35:56–63.

[72] Lichy MP, Plathow C, Schulz-Ertner D, Kauczor HU, Schlemmer HP. Follow-up gliomas after radiotherapy: 1H MR spectroscopic imaging for increasing diagnostic accuracy. Neuroradiology 2005;47:826–34.

[73] Weybright P, Sundgren PC, Maly P, Hassan DG, Nan B, Rohrer S, et al. Differentiation between brain tumor recurrence and radiation injury using MR spectroscopy. Am J Roentgenol 2005;185:1471–6.

[74] Hattingen E, Bahr O, Rieger J, Blasel S, Steinbach J, Pilatus U. Phospholipid metabolites in recurrent glioblastoma: In vivo markers detect different tumor phenotypes before and under antiangiogenic therapy. PLoS One 2013; 8:e56439.

[75] Zeng QS, Li CF, Liu H, Zhen JH, Feng DC. Distinction between recurrent glioma and radiation injury using magnetic resonance spectroscopy in combination with diffusion-weighted imaging. Int J Radiat Oncol Biol Phys 2007;68:151–8.

[76] Rabinov JD, Lee PL, Barker FG, Louis DN, Harsh GR, Cosgrove GR, et al. In vivo 3-T MR spectroscopy in the distinction of recurrent glioma versus radiation effects: Initial experience. Radiology 2002;225:871–9.

[77] Cea V, Sala C, Verpelli C. Antiangiogenic therapy for glioma. J Signal Transduct 2012;2012:15.

[78] Jeon JY, Kovanlikaya I, Boockvar JA, Mao X, Shin B, J KB, et al. Metabolic response of glioblastoma to superselective intra-arterial cerebral infusion of bevacizumab: A proton MR spectroscopic imaging study. Am J Neuroradiol 2012;33: 2095–102.

[79] Ratai E-M, Zhang Z, Snyder BS, Boxerman JL, Safriel Y, McKinstry RC, et al. Magnetic resonance spectroscopy as an early indicator of response to anti-angiogenic therapy in patients with recurrent glioblastoma: RTOG 0625/ACRIN 6677. Neuro Oncol 2013;15:936–44.

[80] Park I, Bok R, Ozawa T, Phillips JJ, James CD, Vigneron DB, et al. Detection of early response to temozolomide treatment in brain tumors using hyperpolarized 13C MR metabolic imaging. J Magn Reson Imaging 2011;33:1284–90.

[81] Bohndiek SE, Kettunen MI, Hu DE, Brindle KM. Hyperpolarized (13)C spectroscopy detects early changes in tumor vasculature and metabolism after VEGF neutralization. Cancer Res 2012;72:854–64.